



Computing Minkowski Sum of Periodic Surface Models

Yan Wang

University of Central Florida, wangyan@mail.ucf.edu

ABSTRACT

Recently we proposed a periodic surface model to assist geometric construction in computer-aided nano-design. This implicit surface model helps create super-porous nano structures parametrically and support crystal packing. In this paper, we study construction methods of Minkowski sums for periodic surfaces. A numerical approximation approach based on the Chebyshev polynomials is developed and can be applied in the formulations of surface normal direction matching and volume translations.

Keywords: implicit/periodic surface, Minkowski sum, computer-aided nano-design.
DOI: 10.3722/cadaps.2009.825-837

1. INTRODUCTION

With the observation that hyperbolic surfaces exist in nature ubiquitously and periodic features are common in condensed materials, we recently proposed an implicit surface modeling approach, periodic surface (PS), to represent geometric structures at nano scales [1,2]. Periodic surfaces are either loci or foci. Loci surfaces are fictional continuous surfaces that pass through discrete particles in 3D space such as in crystals, whereas foci surfaces can be looked as isosurfaces of potential or density in which discrete particles are enclosed. The surface model allows for parametric construction from atomic scale to meso scale. Reconstruction of loci surfaces from crystals [3] and complexity control [4] were also studied. In this paper, we study the Minkowski sum of PS models. Minkowski sums have been widely applied in computer-aided design (CAD), computer-aided manufacturing (CAM), robotic motion and assembly planning, computer graphics, etc. [5,6].

Let \mathbb{A} and \mathbb{B} be two objects in Euclidean space ($\mathbb{A} \subset \mathbb{R}^n$ and $\mathbb{B} \subset \mathbb{R}^n$). The Minkowski sum of \mathbb{A} and \mathbb{B} is generally defined as $\mathbb{A} \oplus \mathbb{B} := \{\mathbf{a} + \mathbf{b} \mid \mathbf{a} \in \mathbb{A} \text{ and } \mathbf{b} \in \mathbb{B}\}$. Minkowski sum is commutative. The sum and union are distributive. However, the sum and intersection are subdistributive. That is, $(\mathbb{X} \cap \mathbb{Y}) \oplus \mathbb{B} = \mathbb{B} \oplus (\mathbb{X} \cap \mathbb{Y}) \subseteq (\mathbb{X} \oplus \mathbb{B}) \cap (\mathbb{Y} \oplus \mathbb{B})$, $(\mathbb{X} \cup \mathbb{Y}) \oplus \mathbb{B} = \mathbb{B} \oplus (\mathbb{X} \cup \mathbb{Y}) = (\mathbb{X} \oplus \mathbb{B}) \cup (\mathbb{Y} \oplus \mathbb{B})$. The Minkowski sum of two convex sets is convex. In a special case, when one of the two objects is a sphere, the Minkowski sum is an offset operation.

Minkowski sum is also closely related to convolution of curves or surfaces. If the boundaries of \mathbb{A} and \mathbb{B} are denoted as $\partial\mathbb{A}$ and $\partial\mathbb{B}$ respectively, the convolution operator $*$ is defined as $\partial\mathbb{A} * \partial\mathbb{B} := \{\mathbf{a} + \mathbf{b} \mid \mathbf{a} \in \partial\mathbb{A}, \mathbf{b} \in \partial\mathbb{B}, \mathbf{N}_a \parallel \mathbf{N}_b\}$, where \mathbf{N}_a and \mathbf{N}_b are the two parallel normal vectors of the boundary surfaces $\partial\mathbb{A}$ and $\partial\mathbb{B}$ at positions \mathbf{a} and \mathbf{b} respectively. The problem of computing the Minkowski sum boundary $\partial(\mathbb{A} \oplus \mathbb{B})$ can be transformed to the problem of computing the convolution between $\partial\mathbb{A}$ and $\partial\mathbb{B}$ because of $\partial(\mathbb{A} \oplus \mathbb{B}) \subseteq \partial\mathbb{A} * \partial\mathbb{B}$. That is, the boundary of the Minkowski sum of

two regions is a subset of the convolution of the two boundaries of the two regions. The boundary of Minkowski sum thus can be derived from the convolution by identifying and removing those segments that lie in the interior of the set.

In computer-aided nano-design, interactive shape manipulation and simulation also require the operation of Minkowski sum. For instance, it can be used to append detailed structures, where small-scale features are added on basic crystal features [7,8]. It is also a very useful tool to study imaging, metrology, path planning in assembly, etc. In this paper, we study Minkowski sums of PS models. A computational approach to generate surfaces based on Chebyshev polynomials is developed, which is applied to surface normal match in convolutions and volume translation in Minkowski sums. In the remainder of the paper, Section 2 gives a brief review of related work in Minkowski sum and convolution of parametric and implicit curves and surfaces. Section 3 gives an overview of the PS model. Section 4 describes the formulation of surface normal matching of periodic surfaces. Section 5 presents the volume translation formulation of Minkowski sums for PS models.

2. SURFACE CONVOLUTION, MINKOWSKI SUMS AND OFFSET

Minkowski sum has been studied extensively in the fields of CAD/CAM and robotics, particularly for geometries with polyhedral representations. Here we only give a brief overview of recent work on parametric and implicit surface models. For two parametric surfaces $\mathbf{a}(u,v)$ and $\mathbf{b}(s,t)$, a reparameterization process can be conducted to find the convolution based on the relationship of parallel normal vectors. If a mapping $(s,t) \mapsto (u(s,t),v(s,t))$ which maintains the parallelism can be found, then the convolution $\mathbf{a}(u(s,t),v(s,t)) * \mathbf{b}(s,t)$ can be constructed by tracing the correspondence between parameters. For some special curves and surfaces, closed-form rational convolutions are available. For instance, the closed-form reparameterization for convolutions between ruled surfaces can be derived [9]. Similarly, revolution surfaces with monotone slope profile curves have explicit reparameterization and can be computed efficiently [10]. Rational convolution surfaces can be obtained between linear normal surfaces and generic rational surfaces [11,12,13].

Offset is a special case of Minkowski sum. The offset of a surface $\mathbf{a}(u,v)$ at a distance d is $\mathbf{a}_d(u,v) = \mathbf{a}(u,v) + d\mathbf{n}(u,v)$ where $\mathbf{n}(u,v)$ is the unit normal vector of \mathbf{a} . The sufficient and necessary condition for $\mathbf{a}_d(u,v)$ to be rational is that $\mathbf{n}(u,v)$ is rational [14,15]. Rational offsets are observed in some special surfaces. For instance, the offsets of Pythagorean-Hodograph curves are rational [16,17]. The offsets of parabola [18] and sinusoidal spiral p-Bézier curves [19] also have rational forms. In generalized offsets, the distance is no longer a constant and may vary at different locations, which has various applications. For example, the variable radius offset of cubic Bézier curves with Bézier interpolations of radius can be applied in brush stroke design [20]. Equivolumetric offset with radius as a function of curvature can be applied to achieve cutting with a constant material removal rate [21].

For more general curves and surfaces, different constructing algorithms for Minkowski sums of parametric curves or surfaces have been developed. By the aid of the implicit relation between tangent directions, Farouki et al. [22] segmented parametric curves by inflection points and cusps. The Minkowski sum is constructed by combinations of segments. Lávička and Bastl [23] used Gröbner bases in reparameterization for rational convolutions. Various algorithms for offsets of parametric surfaces were also developed. Lee et al. [24] generated offset curves by approximating the rolling circle with quadratic Bézier curve segments. Pieggl and Tiller [25] computed offsets of non-uniform rational B-spline curves and surfaces with the steps of sampling, offset, interpolation, and knot removal.

Minkowski sums of regions defined by implicit curves or surfaces have also been studied. In general, the construction of Minkowski sum can be looked as a projection process from a hyperspace to Euclidean space. Since the Minkowski sum between two regions $\mathbb{A} \subset \mathbb{R}^n$ and $\mathbb{B} \subset \mathbb{R}^n$ can be generated by sweeping or translating \mathbb{B} with its origin kept in region \mathbb{A} , a family of \mathbb{B} 's is created as a superset in the hyperspace $\mathbb{R}^n \times \mathbb{R}^n$ with the Euclidean and translation subspaces. If the union of the superset is projected back to the Euclidean space, the generated envelope is the Minkowski sum. Bajaj and Kim

[26] developed generic algorithms to compute convolution for both parametric and implicit curves based on the normal direction constraint. The projection was then achieved by eliminating parameters or variables with resultants. Kaul and Farouki [27] constructed the Minkowski sum between an implicit curve $f(x, y) = 0$ and a parametric curve $(X(t), Y(t))$. The projection was done by finding the resultant of $f(x, y) = 0$ and $\partial f(x - X(t), y - Y(t)) / \partial t = 0$ so that the parameter t is removed. Pasko et al. [28] formulated Minkowski sums between implicit surfaces defined by R-functions [29,30]. The projection was achieved by satisfying the necessary condition of maximum projections globally.

In this paper, we develop two Minkowski sum construction methods for the PS model, which was recently proposed to represent nano-scale geometries, as introduced in Section 3.

3. PERIODIC SURFACE

The periodic surface model has the implicit form and is defined as

$$\psi(\mathbf{r}) = \sum_{l=1}^L \sum_{m=1}^M \mu_{lm} \cos(2\pi \kappa_l (\mathbf{p}_m^T \cdot \mathbf{r})) = 0 \quad (3.1)$$

where κ_l is the *scale parameter*, $\mathbf{p}_m = [a_m, b_m, c_m, d_m]^T$ is a *basis vector*, such as one of

$$\{\mathbf{e}_0, \mathbf{e}_1, \mathbf{e}_2, \mathbf{e}_3, \mathbf{e}_4, \mathbf{e}_5, \mathbf{e}_6, \mathbf{e}_7, \mathbf{e}_8, \mathbf{e}_9, \mathbf{e}_{10}, \mathbf{e}_{11}, \mathbf{e}_{12}, \mathbf{e}_{13}, \dots\} = \left\{ \begin{array}{l} \left[\begin{array}{c} 0 \\ 0 \\ 0 \\ 1 \end{array} \right] \left[\begin{array}{c} 1 \\ 0 \\ 0 \\ 1 \end{array} \right] \left[\begin{array}{c} 0 \\ 1 \\ 0 \\ 1 \end{array} \right] \left[\begin{array}{c} 1 \\ 0 \\ 1 \\ 1 \end{array} \right] \left[\begin{array}{c} 1 \\ 1 \\ 1 \\ 1 \end{array} \right] \left[\begin{array}{c} 0 \\ 1 \\ 1 \\ 1 \end{array} \right] \left[\begin{array}{c} 1 \\ 1 \\ 1 \\ 1 \end{array} \right] \left[\begin{array}{c} 1 \\ -1 \\ 0 \\ 1 \end{array} \right] \left[\begin{array}{c} -1 \\ 0 \\ -1 \\ 1 \end{array} \right] \left[\begin{array}{c} 0 \\ 1 \\ 1 \\ 1 \end{array} \right] \left[\begin{array}{c} 1 \\ -1 \\ 1 \\ 1 \end{array} \right] \left[\begin{array}{c} -1 \\ 1 \\ 1 \\ 1 \end{array} \right] \left[\begin{array}{c} 1 \\ 1 \\ -1 \\ 1 \end{array} \right] \left[\begin{array}{c} 1 \\ 1 \\ 1 \\ 1 \end{array} \right] \dots \end{array} \right\} \quad (3.2)$$

which represents a *basis plane* in the Euclidean space \mathbb{R}^3 , $\mathbf{r} = [x, y, z, w]^T$ is the location vector with homogeneous coordinates, and μ_{lm} is the *periodic moment*. We assume $w = 1$ if not explicitly specified. We call $d_m = \mathbf{p}_m^T \cdot \mathbf{r} / \|\mathbf{p}_m\|$ corresponding to the basis plane \mathbf{p}_m as the *projective distance*. The degree of $\psi(\mathbf{r})$ in Eqn.(3.1) is defined as the number of unique vectors in the basis vector set $\{\mathbf{p}_m\}$. The scale of $\psi(\mathbf{r})$ is defined as the number of unique scale parameters in $\{\kappa_l\}$. We can assume scale parameters are natural numbers ($\kappa \in \mathbb{N}$).

Fig. 1 lists some examples of periodic surface models. Triply periodic minimal surfaces, such as P-, D-, G-, and I-WP cubic morphologies that are frequently referred to in chemistry and polymer literature, can be adequately approximated. Besides the cubic phase, other mesophase structures such as spherical micelles, lamellar, rod-like hexagonal phases can also be modeled.

In this paper, we study the Minkowski sums of PS models. Construction methods are developed based on Chebyshev polynomial approximations.

4. MATCHING SURFACE NORMAL DIRECTIONS

In the first formulation, we construct convolution surfaces by matching normal directions. The numerical algorithm is based on polynomial approximations.

4.1 Surface Convolution Formulation

In general, we would like to find a convolution surface ψ between ψ_1 and ψ_2 , i.e., $\psi_1 * \psi_2 = \psi$, where

$$\psi_1(\mathbf{r}_1) = \sum_{l_1=1}^{L_1} \sum_{m_1=1}^{M_1} \mu_{l_1 m_1}^{(1)} \cos(2\pi \kappa_{l_1}^{(1)} (\mathbf{p}_{m_1}^{(1)T} \cdot \mathbf{r}_1)) = 0 \quad (4.1)$$

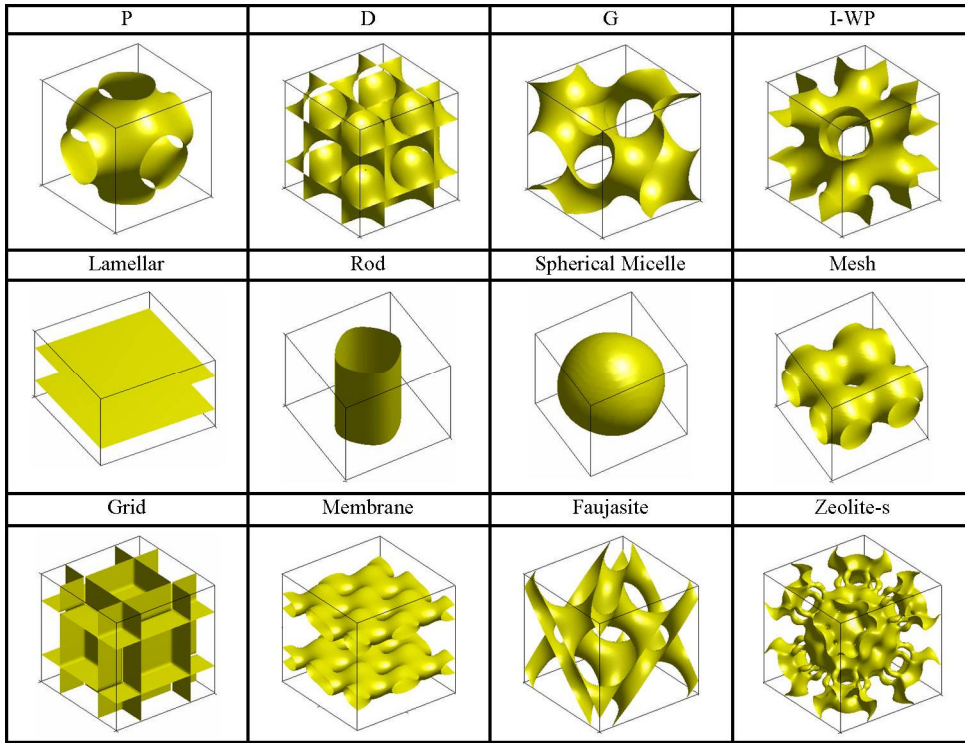


Fig. 1: Periodic surface models of cubic phase and mesophase structures.

$$\psi_2(\mathbf{r}_2) = \sum_{l_2=1}^{L_2} \sum_{m_2=1}^{M_2} \mu_{l_2 m_2}^{(2)} \cos(2\pi \kappa_{l_2}^{(2)} (\mathbf{p}_{m_2}^{(2)T} \cdot \mathbf{r}_2)) = 0 \tag{4.2}$$

A surface normal matching process is required. That is, for any point $\mathbf{r} \in \mathbb{R}^3 \times 1$ on the surface $\psi(\mathbf{r})$, there exists a \mathbf{r}_1 such that the surface normal vectors at the positions \mathbf{r} and $\mathbf{r}_2 = \mathbf{r} - \mathbf{r}_1$ with respect to surfaces $\psi_1(\mathbf{r}_1) = 0$ and $\psi_2(\mathbf{r} - \mathbf{r}_1) = 0$ have the same direction. For the periodic surface in Eqn.(3.1), the surface normal vector is

$$\nabla \psi(\mathbf{r}) = -2\pi \sum_{m=1}^M \left(\sum_{l=1}^L \kappa_l \mu_{lm} \sin(2\pi \kappa_l (\mathbf{p}_m^T \cdot \mathbf{r})) \right) \mathbf{p}_m \tag{4.3}$$

The normal vector is a linear combination of periodic basis vectors with coefficients that are dependent on the position \mathbf{r} . If considered in a Gauss map, as illustrated in Fig. 2(a), a normal vector represented by a point on the unit sphere \mathbb{S}^2 is a combination of basis vectors \mathbf{p}_m 's. In order to ensure a match of normal vectors, one of the two surfaces ψ_1 and ψ_2 should have at least three non-coplanar basis vectors. As illustrated in Fig. 2(b), to find a match of any normal vector $\mathbf{q}^{(2)}$ of ψ_2 , we need at least three basis vectors $\mathbf{p}_1^{(1)}$, $\mathbf{p}_2^{(1)}$, and $\mathbf{p}_3^{(1)}$ of ψ_1 where $\mathbf{p}_1^{(1)} \cdot (\mathbf{p}_2^{(1)} \times \mathbf{p}_3^{(1)}) \neq 0$ such that $\mathbf{q}^{(2)}$ is a linear combination of $\mathbf{p}_1^{(1)}$, $\mathbf{p}_2^{(1)}$, and $\mathbf{p}_3^{(1)}$.

The two constraints

$$\nabla \psi_1(\mathbf{r}_1) \times \nabla \psi_2(\mathbf{r} - \mathbf{r}_1) = 0 \tag{4.4}$$

$$\nabla \psi_1(\mathbf{r}_1) \cdot \nabla \psi_2(\mathbf{r} - \mathbf{r}_1) > 0 \tag{4.5}$$

need to be satisfied to match normal directions. The convolution surface $\psi(\mathbf{r}) = 0$ then can be derived by removing \mathbf{r}_1 in the implicit surface

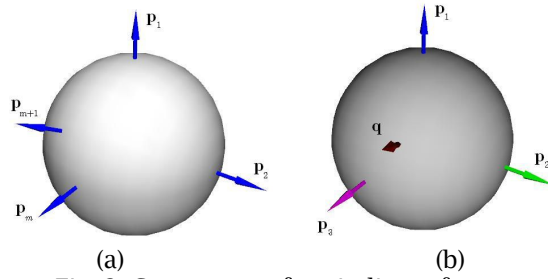


Fig. 2: Gauss map of periodic surfaces.

$$\psi_2(\mathbf{r} - \mathbf{r}_1) = \sum_{l_2=1}^{L_2} \sum_{m_2=1}^{M_2} \mu_{l_2 m_2}^{(2)} \cos\left(2\pi \kappa_{l_2}^{(2)} (\mathbf{p}_{m_2}^{(2)\text{T}} \cdot (\mathbf{r} - \mathbf{r}_1))\right) = 0$$

and rewriting it with respect to \mathbf{r} based on the relations in Eqn.(4.4) and Eqn.(4.5).

To simplify the notation, let

$$\begin{aligned} \gamma_{m_1}^{(1)} &= \sum_{l_1=1}^{L_1} \kappa_{l_1}^{(1)} \mu_{l_1 m_1}^{(1)} \sin\left(2\pi \kappa_{l_1}^{(1)} (\mathbf{p}_{m_1}^{(1)\text{T}} \cdot \mathbf{r}_1)\right) \\ \gamma_{m_2}^{(2)} &= \sum_{l_2=1}^{L_2} \kappa_{l_2}^{(2)} \mu_{l_2 m_2}^{(2)} \sin\left(2\pi \kappa_{l_2}^{(2)} (\mathbf{p}_{m_2}^{(2)\text{T}} \cdot (\mathbf{r} - \mathbf{r}_1))\right) \end{aligned}$$

The constraint of Eqn.(4.4) becomes

$$\sum_{m_1=1}^{M_1} \gamma_{m_1}^{(1)} \mathbf{p}_{m_1}^{(1)} \times \sum_{m_2=1}^{M_2} \gamma_{m_2}^{(2)} \mathbf{p}_{m_2}^{(2)} = 0 \tag{4.6}$$

With $\mathbf{p}_{m_1}^{(1)} = [a_{m_1}^{(1)}, b_{m_1}^{(1)}, c_{m_1}^{(1)}, d_{m_1}^{(1)}]^\text{T}$ and $\mathbf{p}_{m_2}^{(2)} = [a_{m_2}^{(2)}, b_{m_2}^{(2)}, c_{m_2}^{(2)}, d_{m_2}^{(2)}]^\text{T}$, Eqn.(4.6) is rewritten as

$$\begin{cases} \left(\sum_{m_1=1}^{M_1} \gamma_{m_1}^{(1)} b_{m_1}^{(1)} \right) \left(\sum_{m_2=1}^{M_2} \gamma_{m_2}^{(2)} c_{m_2}^{(2)} \right) - \left(\sum_{m_1=1}^{M_1} \gamma_{m_1}^{(1)} c_{m_1}^{(1)} \right) \left(\sum_{m_2=1}^{M_2} \gamma_{m_2}^{(2)} b_{m_2}^{(2)} \right) = 0 \\ \left(\sum_{m_1=1}^{M_1} \gamma_{m_1}^{(1)} a_{m_1}^{(1)} \right) \left(\sum_{m_2=1}^{M_2} \gamma_{m_2}^{(2)} c_{m_2}^{(2)} \right) - \left(\sum_{m_1=1}^{M_1} \gamma_{m_1}^{(1)} c_{m_1}^{(1)} \right) \left(\sum_{m_2=1}^{M_2} \gamma_{m_2}^{(2)} a_{m_2}^{(2)} \right) = 0 \\ \left(\sum_{m_1=1}^{M_1} \gamma_{m_1}^{(1)} a_{m_1}^{(1)} \right) \left(\sum_{m_2=1}^{M_2} \gamma_{m_2}^{(2)} b_{m_2}^{(2)} \right) - \left(\sum_{m_1=1}^{M_1} \gamma_{m_1}^{(1)} b_{m_1}^{(1)} \right) \left(\sum_{m_2=1}^{M_2} \gamma_{m_2}^{(2)} a_{m_2}^{(2)} \right) = 0 \end{cases}$$

Equivalently,

$$\begin{cases} \sum_{m_1=1}^{M_1} \sum_{m_2=1}^{M_2} \gamma_{m_1}^{(1)} \gamma_{m_2}^{(2)} (b_{m_1}^{(1)} c_{m_2}^{(2)} - b_{m_2}^{(2)} c_{m_1}^{(1)}) = 0 \\ \sum_{m_1=1}^{M_1} \sum_{m_2=1}^{M_2} \gamma_{m_1}^{(1)} \gamma_{m_2}^{(2)} (a_{m_1}^{(1)} c_{m_2}^{(2)} - a_{m_2}^{(2)} c_{m_1}^{(1)}) = 0 \\ \sum_{m_1=1}^{M_1} \sum_{m_2=1}^{M_2} \gamma_{m_1}^{(1)} \gamma_{m_2}^{(2)} (a_{m_1}^{(1)} b_{m_2}^{(2)} - a_{m_2}^{(2)} b_{m_1}^{(1)}) = 0 \end{cases}$$

Substituting $\gamma_{m_1}^{(1)}$ and $\gamma_{m_2}^{(2)}$ with their original forms, we need to derive the relationship between \mathbf{r} and \mathbf{r}_1 from

$$\begin{cases} \sum_{m_1=1}^{M_1} \sum_{m_2=1}^{M_2} \sum_{l_1=1}^{L_1} \sum_{l_2=1}^{L_2} \left[\left(b_{m_1}^{(1)} c_{m_2}^{(2)} - b_{m_2}^{(2)} c_{m_1}^{(1)} \right) \kappa_{l_1}^{(1)} \kappa_{l_2}^{(2)} \mu_{l_1 m_1}^{(1)} \mu_{l_2 m_2}^{(2)} \sin \left(2\pi \kappa_{l_1}^{(1)} \left(\mathbf{p}_{m_1}^{(1)T} \cdot \mathbf{r}_1 \right) \right) \sin \left(2\pi \kappa_{l_2}^{(2)} \left(\mathbf{p}_{m_2}^{(2)T} \cdot (\mathbf{r} - \mathbf{r}_1) \right) \right) \right] = 0 \\ \sum_{m_1=1}^{M_1} \sum_{m_2=1}^{M_2} \sum_{l_1=1}^{L_1} \sum_{l_2=1}^{L_2} \left[\left(a_{m_1}^{(1)} c_{m_2}^{(2)} - a_{m_2}^{(2)} c_{m_1}^{(1)} \right) \kappa_{l_1}^{(1)} \kappa_{l_2}^{(2)} \mu_{l_1 m_1}^{(1)} \mu_{l_2 m_2}^{(2)} \sin \left(2\pi \kappa_{l_1}^{(1)} \left(\mathbf{p}_{m_1}^{(1)T} \cdot \mathbf{r}_1 \right) \right) \sin \left(2\pi \kappa_{l_2}^{(2)} \left(\mathbf{p}_{m_2}^{(2)T} \cdot (\mathbf{r} - \mathbf{r}_1) \right) \right) \right] = 0 \\ \sum_{m_1=1}^{M_1} \sum_{m_2=1}^{M_2} \sum_{l_1=1}^{L_1} \sum_{l_2=1}^{L_2} \left[\left(a_{m_1}^{(1)} b_{m_2}^{(2)} - a_{m_2}^{(2)} b_{m_1}^{(1)} \right) \kappa_{l_1}^{(1)} \kappa_{l_2}^{(2)} \mu_{l_1 m_1}^{(1)} \mu_{l_2 m_2}^{(2)} \sin \left(2\pi \kappa_{l_1}^{(1)} \left(\mathbf{p}_{m_1}^{(1)T} \cdot \mathbf{r}_1 \right) \right) \sin \left(2\pi \kappa_{l_2}^{(2)} \left(\mathbf{p}_{m_2}^{(2)T} \cdot (\mathbf{r} - \mathbf{r}_1) \right) \right) \right] = 0 \end{cases} \quad (4.7)$$

A degenerated situation occurs when $b_{m_1}^{(1)} c_{m_2}^{(2)} - b_{m_2}^{(2)} c_{m_1}^{(1)} = 0$, $a_{m_1}^{(1)} c_{m_2}^{(2)} - a_{m_2}^{(2)} c_{m_1}^{(1)} = 0$, and $a_{m_1}^{(1)} b_{m_2}^{(2)} - a_{m_2}^{(2)} b_{m_1}^{(1)} = 0$ in Eqn.(4.7) for all $m_1 = 1, \dots, M_1$ and $m_2 = 1, \dots, M_2$. This happens when, for example, (1) $a_{m_1}^{(1)} = \alpha a_{m_2}^{(2)}$, $b_{m_1}^{(1)} = \alpha b_{m_2}^{(2)}$, and $c_{m_1}^{(1)} = \alpha c_{m_2}^{(2)}$ for some $\alpha \in \mathbb{R}$ ($\alpha \neq 0$) and any m_1 and m_2 ; (2) $a_{m_1}^{(1)} = b_{m_1}^{(1)} = c_{m_1}^{(1)}$ and $a_{m_2}^{(2)} = b_{m_2}^{(2)} = c_{m_2}^{(2)}$ for all m_1 and m_2 ; (3) $a_{m_1}^{(1)} = -b_{m_1}^{(1)} = c_{m_1}^{(1)}$ and $a_{m_2}^{(2)} = -b_{m_2}^{(2)} = c_{m_2}^{(2)}$ for all m_1 and m_2 ; and so on. In these degenerated situations, Eqn.(4.7) has no solutions. Convolution surfaces can only be found for some special cases. For instance,

- When $M_1 = M_2 = 1$, lamellar surfaces $\psi_1(\mathbf{r}_1) = \sum_{l_1=1}^{L_1} \mu_{l_1}^{(1)} \cos(2\pi \kappa_{l_1}^{(1)} (\mathbf{p}^{(1)T} \cdot \mathbf{r}_1)) = 0$ and $\psi_2(\mathbf{r}_2) = \sum_{l_2=1}^{L_2} \mu_{l_2}^{(2)} \cos(2\pi \kappa_{l_2}^{(2)} (\mathbf{p}^{(2)T} \cdot \mathbf{r}_2)) = 0$ have only one basis vector $\mathbf{p}^{(1)}$ and $\mathbf{p}^{(2)}$ respectively, there is no convolution surface $\psi = \psi_1 * \psi_2$ unless $\mathbf{p}^{(1)} \times \mathbf{p}^{(2)} = 0$. The convolution surface is a lamellar surface.
- When $M_1 = 1$ and $M_2 = 2$, a lamellar surface $\psi_1 = 0$ has one basis vector $\mathbf{p}^{(1)}$, and a prism alike surface $\psi_2 = 0$ has two basis vectors $\mathbf{p}_1^{(2)}$ and $\mathbf{p}_2^{(2)}$. The necessary condition that a convolution surface exists is $\mathbf{p}^{(1)} \cdot (\mathbf{p}_1^{(2)} \times \mathbf{p}_2^{(2)}) = 0$. The convolution surface is a lamellar surface.

Remark The convolution surface between a lamellar surface and another PS surface is always a lamellar surface, if there exists one.

The convolution associated with lamellar surfaces is the simplest case, which is also of special interest due to its usage in feature based crystal constructions [7,8]. The convolution surface between a lamellar surface and another PS surface can be constructed by searching the points on the PS surface that has the same normal direction as the lamellar surface.

Theoretically, solving Eqn.(4.7), we can derive an algebraic relation $\mathbf{r}_1 = \boldsymbol{\rho}(\mathbf{r})$. Then $\psi_2(\mathbf{r} - \boldsymbol{\rho}(\mathbf{r})) = 0$ is the Minkowski sum between ψ_1 and ψ_2 . However, this is not practical due to the computational complexity. A closed-form nonlinear relationship $\boldsymbol{\rho}$ is not easy to derive. Therefore, we develop a local approximation method based on the Chebyshev polynomials so that the resultant methods in symbolic computation can be applied in deriving $\psi_2(\mathbf{r} - \boldsymbol{\rho}(\mathbf{r})) = 0$. This is described in Section 4.2.

4.2 Polynomial Approximation

With the Chebyshev polynomials of the first kind

$$T_j(x) = \cos(j \cos^{-1} x) \quad x \in [-1, 1] \quad (4.8)$$

the expansion of a locally continuous function $f(x)$ within the domain $x \in [-1, 1]$ is

$$f(x) = \frac{1}{2} c_0 + \sum_{j=1}^{\infty} c_j T_j(x) \quad x \in [-1, 1] \quad (4.9)$$

where

$$c_j = \frac{2}{\pi} \int_{-1}^1 \frac{1}{\sqrt{1-x^2}} f(x) T_j(x) dx \quad j = 0, 1, 2, \dots \tag{4.10}$$

The Chebyshev polynomials also have a recursive relation $T_{n+1} = 2xT_n - T_{n-1}$ for ease of computation, where $T_0 = 1$ and $T_1 = x$, and an identity relation $T_i \cdot T_j = (T_{|i-j|} + T_{i+j})/2$.

We consider the Minkowski sum of $\psi_1(\mathbf{r}_1) = 0$ and $\psi_2(\mathbf{r}_2) = 0$ within two domains \mathbb{D}_1 and \mathbb{D}_2 . The Chebyshev polynomials can be used to approximate ψ_2 and Eqn.(4.7) within the domains. Notice that translation and scaling are required in order to map the spatial domain to the Chebyshev parameter range of $[-1, 1]$. Then the resultant from the four equations is the convolution envelope surface. We illustrate the computation by the following example of surface offset.

Example 1 Given a P surface $\psi_1(x_1, y_1, z_1) = \cos(2\pi x_1) + \cos(2\pi y_1) + \cos(2\pi z_1) = 0$, we would like to find its offset surface with a distance ratio r that is proportional to the local surface normal vector. The surface normal vector of ψ_1 at (x_1, y_1, z_1) is $\nabla\psi_1 = [-2\pi \sin(2\pi x_1), -2\pi \sin(2\pi y_1), -2\pi \sin(2\pi z_1)]^T$. We need to find relations $x_1 = \rho_1(x, y, z)$, $y_1 = \rho_2(x, y, z)$, and $z_1 = \rho_3(x, y, z)$ from

$$\begin{cases} x = x_1 - r \cdot 2\pi \sin(2\pi x_1) \\ y = y_1 - r \cdot 2\pi \sin(2\pi y_1) \\ z = z_1 - r \cdot 2\pi \sin(2\pi z_1) \end{cases} \tag{4.11}$$

so that $\psi(x, y, z) = 0$ can be found by substituting x_1 , y_1 , and z_1 in $\psi_1(x_1, y_1, z_1) = 0$ with ρ_1 , ρ_2 , and ρ_3 respectively.

Let $X_1 = \cos(2\pi x_1)$, $Y_1 = \cos(2\pi y_1)$, and $Z_1 = \cos(2\pi z_1)$. Eqn.(4.11) becomes

$$\begin{cases} f_1(X_1) = (C_1 \pm 1/2\pi \cos^{-1} X_1) \pm r \cdot 2\pi \sqrt{1 - X_1^2} - x = 0 \\ f_2(Y_1) = (C_2 \pm 1/2\pi \cos^{-1} Y_1) \pm r \cdot 2\pi \sqrt{1 - Y_1^2} - y = 0 \\ f_3(Z_1) = (C_3 \pm 1/2\pi \cos^{-1} Z_1) \pm r \cdot 2\pi \sqrt{1 - Z_1^2} - z = 0 \end{cases}$$

The constants C_j ($j = 1, 2, 3$) and \pm signs are domain-dependent. For instance, considering a subdomain where $0 \leq x_1 \leq 0.25$, $0 \leq y_1 \leq 0.25$, and $0 \leq z_1 \leq 0.25$, we have $C_1 = C_2 = C_3 = 0$ and $f_1(X_1) = (1/2\pi \cos^{-1} X_1) - r \cdot 2\pi \sqrt{1 - X_1^2} - x$, because $\sin(2\pi x_1) \geq 0$. f_2 and f_3 are similar. When $r = 0.01$, the Chebyshev polynomial approximations of f_1 , f_2 and f_3 with degree of three in this subdomain are

$$\begin{cases} f_1^{(3)}(X_1) = -0.0245896X_1^3 + 0.0312159X_1^2 - 0.159148X_1 + 0.187168 - x \\ f_2^{(3)}(Y_1) = -0.0245896Y_1^3 + 0.0312159Y_1^2 - 0.159148Y_1 + 0.187168 - y \\ f_3^{(3)}(Z_1) = -0.0245896Z_1^3 + 0.0312159Z_1^2 - 0.159148Z_1 + 0.187168 - z \end{cases} \tag{4.12}$$

Fig. 3 compares the function $(1/2\pi \cos^{-1} X) - r \cdot 2\pi \sqrt{1 - X^2}$ with the polynomial approximation $-0.0245896X^3 + 0.0312159X^2 - 0.159148X + 0.187168$ within the subdomain $X \in [0, 1]$.

From the three equations from Eqn.(4.12) along with the original surface $\psi_1 = X_1 + Y_1 + Z_1 = 0$, we eliminate X_1 , Y_1 , and Z_1 by recursively computing the resultants from the determinants of Sylvester matrices. The final resultant $\psi(x, y, z) = 0$ contains 184 monomials. Fig. 4 shows the polynomial approximations in four subdomains, where the red are the original surfaces and the yellow are the

offsets. In Fig. 5, the polynomial approximations in the subdomain $0 \leq x_1 \leq 0.5$, $0 \leq y_1 \leq 0.5$, and $0 \leq z_1 \leq 0.5$ with degrees of three and four are compared.

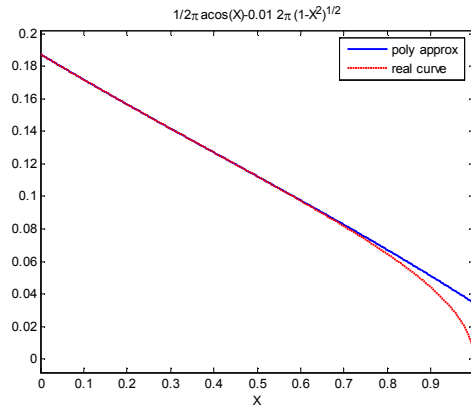


Fig. 3: Local approximation by Chebyshev polynomials in Example 1.

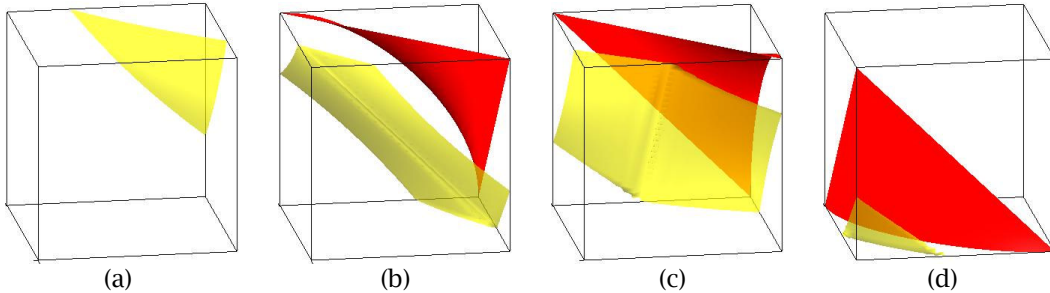


Fig. 4: P surface offset with Chebyshev polynomial approximations in four subdomains in Example 1. (a) $x \in [0, 0.25], y \in [0, 0.25], z \in [0, 0.25]$; (b) $x \in [0, 0.25], y \in [0.25, 0.5], z \in [0, 0.25]$; (c) $x \in [0.25, 0.5], y \in [0, 0.25], z \in [0, 0.25]$; (d) $x \in [0.25, 0.5], y \in [0.25, 0.5], z \in [0, 0.25]$.

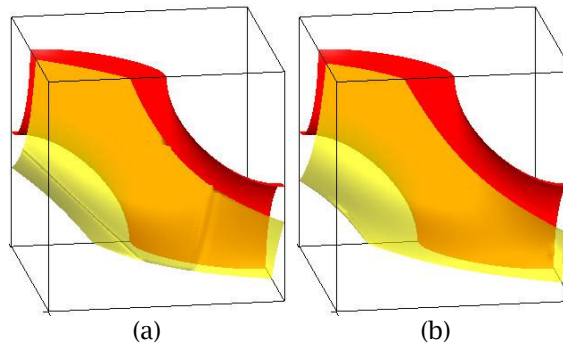


Fig. 5: Polynomial approximations with degrees of three and four. (a) $-0.0271349X_1^3 + 0.0325528X_1^2 - 0.159319X_1 + 0.187171 - x$; (b) $-0.00828778X_1^4 - 0.0188471X_1^3 + 0.0299628X_1^2 - 0.159060X + 0.187167 - x$.

Notice that the approximation error can be reduced by either increasing the degrees of polynomials or subdividing domains. It is well known that a good local approximation of a continuous function by polynomials can always be obtained by increasing the degree, stated as follows.

Theorem 1 (Weierstrass Theorem) For any given $f(x)$ that is continuous in the domain $x \in [a, b]$ and for any given $\varepsilon > 0$, there exists a polynomial p_n for some sufficiently large n such that $\|f - p_n\|_\infty < \varepsilon$ where $\|\cdot\|_\infty$ denotes L_∞ norm.

The above local polynomial approximation can be extended to the criteria of L_p norms for any $p \geq 1$, since L_p norms are bounded by L_∞ norm. In general, $\|z\|_{p_1} \leq C \|z\|_{p_2}$ with $1 \leq p_1 \leq p_2 \leq \infty$ and a finite constant C for any z in a L_{p_2} subspace. Chebyshev polynomials give the best L_∞ or minimax approximations of continuous functions based on the criterion of L_∞ norm due to the following alternation theorem.

Theorem 2 (Alternation Theorem [31, Theorem 3.4]) For any continuous $f(x)$ in the domain $x \in [a, b]$, the sufficient and necessary condition that a unique minimax polynomial approximation $p_n(x)$ with degree of n exists is that there are at least $n + 2$ points $x_i \in [a, b]$ where $\varepsilon_n(x) = f(x) - p_n(x)$ attains its maximum absolute value, i.e. $\max_{x \in [a, b]} |\varepsilon_n(x)| = |\varepsilon_n(x_i)|$ for $(i = 1, \dots, n + 2)$, but with alternating \pm signs.

The Chebyshev polynomial $T_n(x)$ has $n + 1$ extrema (+1 or -1) at $x_i = \cos(i\pi/n)$ where $(i = 0, 1, \dots, n)$. Therefore, Chebyshev polynomials give best approximations of continuous functions in terms of L_∞ norm. In addition, with the inner product between f and g defined as

$$\langle f, g \rangle = \int_{-1}^1 \frac{1}{\sqrt{1-x^2}} f(x)g(x)dx$$

which is used in Eqn.(4.10), $T_n(x)$'s are orthogonal polynomials, with the corresponding L_2 norm as $\|f\|_2 = \sqrt{\langle f, f \rangle}$. The approximation error is

$$\|\varepsilon_n\|_2^2 = \langle f - p_n, f - p_n \rangle = \left\langle \sum_{j=n+1}^{\infty} c_j T_j(x), \sum_{j=n+1}^{\infty} c_j T_j(x) \right\rangle = \sum_{j=n+1}^{\infty} c_j^2$$

The convergence rate depends on the smoothness of $f(x)$, asserted as follows.

Lemma 3 [3]. If $f(x)$ is d times continuously differentiable, the coefficient c_n in the Chebyshev approximation of $f(x)$ as in Eqn.(4.10) converges at a rate of $O(n^{-d})$.

The PS model is infinitely differentiable. Therefore the Chebyshev approximation of PS models has the advantage of fast convergence. In Example 1, $\cos^{-1}(X)$ and $\sqrt{1-X^2}$ are also infinitely differentiable in domain $X \in (-1, 1)$. Fig. 6 illustrates the convergence of Chebyshev polynomial approximations.

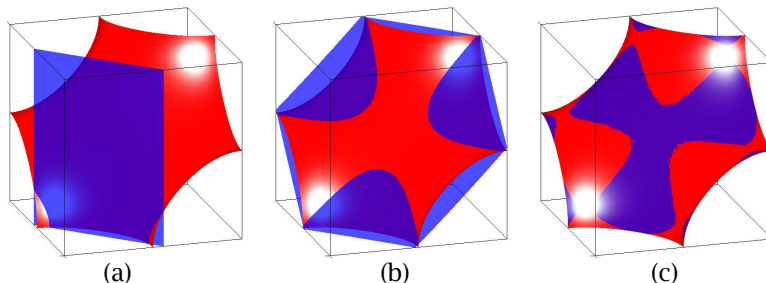


Fig. 6: Convergence of polynomial approximations (in blue) towards P surface (in red) in domain $x \in [-0.5, 0], y \in [-0.5, 0], z \in [-0.5, 0]$. (a) degree of 1; (b) degree of 2; (c) degree of 3.

5. VOLUME TRANSLATION

We can construct the Minkowski sum based on the volumetric information of PS models. In the second formulation, the Minkowski sum is found by translating volumes and projecting from the hyperspace to the Euclidean space.

5.1 Volume Translation Formulation

Consider two domains $\psi_1(\mathbf{r}_1) \leq 0$ and $\psi_2(\mathbf{r}_2) \leq 0$ in Euclidean space \mathbb{R}^3 . The Minkowski sum $\psi(\mathbf{r}) \leq 0$ can be regarded as the union of translated ψ_2 's with the translation vectors in ψ_1 . If considered a six-dimensional hyperspace $\mathbb{R}^3 \times \mathbb{R}^3$, the intersection between $\psi_1(\mathbf{r}_1, \mathbf{r} - \mathbf{r}_1)$ and $\psi_2(\mathbf{r}_1, \mathbf{r} - \mathbf{r}_1)$, where $\mathbf{r}_1 + \mathbf{r}_2 = \mathbf{r}$, can be projected back to 3D Euclidean space. The resulted projection in Euclidean space is $\psi(\mathbf{r}) \leq 0$. The intersection between $\psi_1(\mathbf{r}_1, \mathbf{r} - \mathbf{r}_1) \leq 0$ and $\psi_2(\mathbf{r}_1, \mathbf{r} - \mathbf{r}_1) \leq 0$ is $\psi(\mathbf{r}_1, \mathbf{r} - \mathbf{r}_1) = \max[\psi_1(\mathbf{r}_1), \psi_2(\mathbf{r} - \mathbf{r}_1)] \leq 0$.

The direct computation process is straightforward. In a specified domain \mathbb{D}_1 , the union of the translated ψ_2 with ψ_1 is recorded if the intersection between the two is not empty. The envelope of all unions will be the Minkowski sum. The construction algorithm is listed in Fig. 7. Some examples are shown in Fig. 8.

```

k = 0;
 $\psi^{(k)}(\mathbf{r}) = \psi_1(\mathbf{r});$ 
FOR all  $\mathbf{r}_1 \in \mathbb{D}_1$ 
    k = k + 1;
    IF there is a  $\mathbf{r} \in \mathbb{D}_1$  such that  $\max(\psi_1(\mathbf{r}), \psi_2(\mathbf{r} - \mathbf{r}_1)) < 0$ 
        THEN  $\psi^{(k)}(\mathbf{r}) = \min(\min(\psi_1(\mathbf{r}), \psi_2(\mathbf{r} - \mathbf{r}_1)), \psi^{(k-1)}(\mathbf{r}));$ 
    END IF
END FOR
Return  $\psi^{(k)}(\mathbf{r});$ 

```

Fig. 7: Volume translation algorithm.

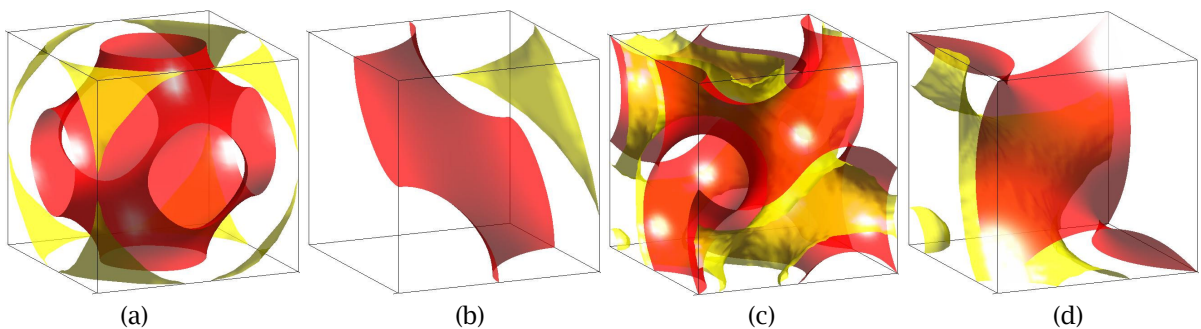


Fig. 8: Some examples of Minkowski sums constructed based on volume translations. (a) P surface and Micelle $8 - \cos(2\pi x) - \cos(2\pi y) - \cos(2\pi z) = 0$ in domain $x \in [-1, 0], y \in [-1, 0], z \in [-1, 0]$ (grid size: $25 \times 25 \times 25$); (b) P surface and Micelle in domain $x \in [-0.5, 0], y \in [-0.5, 0], z \in [-0.5, 0]$ (grid size: $25 \times 25 \times 25$); (c) G surface and Sphere $x^2 + y^2 + z^2 - 0.0025 = 0$ in domain $x \in [-1, 0], y \in [-1, 0], z \in [-1, 0]$ (grid size: $50 \times 50 \times 50$); (d) G surface and Sphere in domain $x \in [-0.5, 0], y \in [-0.5, 0], z \in [-0.5, 0]$ (grid size: $50 \times 50 \times 50$).

The volume translation can also be formulated as an optimization problem. Since we try to find the union of the moving region $\psi_2(\mathbf{r} - \mathbf{r}_1) \leq 0$ within the region $\psi_1(\mathbf{r}_1) \leq 0$, the Minkowski sum $\psi(\mathbf{r}) \leq 0$ is equivalent to the optimal solution of the minimization problem

$$\underset{\mathbf{r}_1 \in \mathbb{D}_1}{\text{MIN}} \left\{ \max[\psi_1(\mathbf{r}_1), \psi_2(\mathbf{r} - \mathbf{r}_1)] \right\} \quad (5.1)$$

Because the objective function in Eqn.(5.1) is not C^1 continuous due to the \max function, we divide it into two equivalent sub problems as

$$\begin{aligned} & \underset{x_1, y_1, z_1}{\text{MIN}} \left\{ \psi_1(x_1, y_1, z_1) \right\} \\ & \text{subject to: } \psi_1(x_1, y_1, z_1) \geq \psi_2(x - x_1, y - y_1, z - z_1) \end{aligned} \quad (5.2)$$

and

$$\begin{aligned} & \underset{x_1, y_1, z_1}{\text{MIN}} \left\{ \psi_2(x - x_1, y - y_1, z - z_1) \right\} \\ & \text{subject to: } \psi_1(x_1, y_1, z_1) \leq \psi_2(x - x_1, y - y_1, z - z_1) \end{aligned} \quad (5.3)$$

The respective necessary conditions of the optimality are

$$\begin{aligned} \frac{\partial \psi_1}{\partial x_1} + \lambda_1 \left[\frac{\partial \psi_2}{\partial x_1} - \frac{\partial \psi_1}{\partial x_1} \right] &= 0 \\ \frac{\partial \psi_1}{\partial y_1} + \lambda_2 \left[\frac{\partial \psi_2}{\partial y_1} - \frac{\partial \psi_1}{\partial y_1} \right] &= 0 \\ \frac{\partial \psi_1}{\partial z_1} + \lambda_3 \left[\frac{\partial \psi_2}{\partial z_1} - \frac{\partial \psi_1}{\partial z_1} \right] &= 0 \\ \lambda_1 [\psi_2 - \psi_1] &= 0 \\ \lambda_2 [\psi_2 - \psi_1] &= 0 \\ \lambda_3 [\psi_2 - \psi_1] &= 0 \end{aligned} \quad (5.4)$$

and

$$\begin{aligned} \frac{\partial \psi_2}{\partial x_1} + \lambda'_1 \left[\frac{\partial \psi_1}{\partial x_1} - \frac{\partial \psi_2}{\partial x_1} \right] &= 0 \\ \frac{\partial \psi_2}{\partial y_1} + \lambda'_2 \left[\frac{\partial \psi_1}{\partial y_1} - \frac{\partial \psi_2}{\partial y_1} \right] &= 0 \\ \frac{\partial \psi_2}{\partial z_1} + \lambda'_3 \left[\frac{\partial \psi_1}{\partial z_1} - \frac{\partial \psi_2}{\partial z_1} \right] &= 0 \\ \lambda'_1 [\psi_1 - \psi_2] &= 0 \\ \lambda'_2 [\psi_1 - \psi_2] &= 0 \\ \lambda'_3 [\psi_1 - \psi_2] &= 0 \end{aligned} \quad (5.5)$$

Therefore, the resultant found from either Eqn.(5.4) or Eqn.(5.5) along with $\psi_2(x - x_1, y - y_1, z - z_1) = 0$ is the Minkowski sum of two PS models for some given subdomains.

5.2 Polynomial Approximations

To compute resultant, we also apply polynomial approximations. Similar to Section 4.2, approximations can be achieved based on the Chebyshev polynomials as in Eqn.(4.8). Here, we only approximate ψ_1 and ψ_2 , as in Eqn.(5.4) and Eqn.(5.5). The following example is used to illustrate the process.

Example 2 We would like to construct the Minkowski sum between a P surface $\psi_1(x_1, y_1, z_1) = \cos(2\pi x_1) + \cos(2\pi y_1) + \cos(2\pi z_1) = 0$ and a spherical micelle

$\psi_2(x_2, y_2, z_2) = 4 - 3 \cos(2\pi x_2) - 3 \cos(2\pi y_2) - 3 \cos(2\pi z_2) = 0$ within the subdomains $x_1 \in [-0.5, 0], y_1 \in [-0.5, 0], z_1 \in [-0.5, 0]$ and $x_2 \in [-0.5, 0], y_2 \in [-0.5, 0], z_2 \in [-0.5, 0]$. The two surfaces in the subdomain are shown in Fig. 6, where the P surface is in red color, and the spherical micelle is in blue.

We construct local linear approximations of ψ_1 and ψ_2 based on Chebyshev polynomials. They are $3.400945 + 4.534593x_1 + 4.534593y_1 + 4.534593z_1 = 0$ and $-6.202834 - 13.603778(x - x_1) - 13.603778(y - y_1) - 13.603778(z - z_1) = 0$ respectively. The Minkowski sum of the two regions are constructed based on Eqn.(5.4). Eliminating the Lagrange multipliers λ_1, λ_2 , and λ_3 we derive the resultant, which is $337.342041 + 279.728110x + 279.728110y + 279.728110z = 0$, as shown in Fig. 9 in yellow.

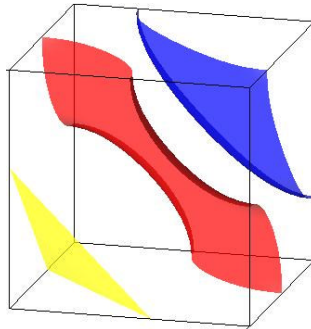


Fig. 9: The P surface (red), spherical micelle surface (blue), and approximated Minkowski sum (yellow) in Example 2

The linear approximation in the above example is easy to compute. However, if the degrees of polynomials increase, the computation will become much more expensive. In this case, a direct computation of translational volumes is more favorable.

6. SUMMARY

In this paper, we study Minkowski sum construction methods for the recently developed PS model. A numerical approximation approach based on Chebyshev polynomials is formulated, which can be applied to both matching surface normal directions and volume translations. The polynomials provide good approximations of PS models. Symbolic resultant computation then can be applied to eliminate variables, and implicit forms can be derived. However, the major issue of this approach is the cost of symbolic computation when the degrees of polynomials increase. This is even more significant compared to the direct computation of volume translation. Future study may include other construction approaches such as domain subdivision and sample based surface reconstruction so that accuracy can be improved without increasing degrees.

7. ACKNOWLEDGEMENTS

This work is supported in part by the NSF Grant CMMI-0645070.

8. REFERENCES

- [1] Wang, Y.: Geometric modeling of nano structures with periodic surfaces, Proc. Geometric Modeling & Processing 2006, In Lecture Notes in Computer Science, ed. by M.-S. Kim and K. Shimada, Vol.4077, 2006, pp.343-356.
- [2] Wang, Y.: Periodic surface modeling for computer aided nano design, Computer-Aided Design, 39(3), 2007, 179-189.
- [3] Wang, Y.: Loci periodic surface reconstruction from crystals, Computer-Aided Design & Applications, 4(1-4), 2007, 437-447.
- [4] Wang, Y.: Degree elevation and reduction of periodic surfaces, Computer-Aided Design & Applications, 5(6), 2008, 841-854.

- [5] Elber, G.; Lee, I.-K.; Kim, M.-S.: Comparing offset curve approximation methods, *IEEE Computer Graphics & Applications*, 17(3), 1997, 62-71.
- [6] Maekawa, T.: An overview of offset curves and surfaces, *Computer-Aided Design*, 31(3), 1999, 165-173.
- [7] Qi, C.; Wang, Y.: Feature-based crystal construction in computer-aided nano-design, *Proc. 2008 ASME International Design Engineering Technical Conferences & Computer and Information in Engineering Conference (IDETC/CIE2008)*, Paper No. DETC2008-49650
- [8] Qi, C.; Wang, Y.: Feature-based crystal construction with periodic surfaces, *Computer-Aided Design*, 2009 (submitted)
- [9] Mühlthaler, H.; Pottmann, H.: Computing the Minkowski sum of ruled surfaces, *Graphical Models*, 65(6), 2003, 369-384.
- [10] Seong, J.-K.; Kim, M.-S.; Sugihara, K.: The Minkowski sum of two simple surfaces generated by slope-monotone closed curves, *IEEE Proc. Geometric Modeling & Processing 2002*, pp.33-42.
- [11] Sampoli, M. L.; Peternell, M.; Jüttler, B.: Rational surfaces with linear normals and their convolutions with rational surfaces, *Computer Aided Geometric Design*, 23(2), 2006, 179-192.
- [12] Peternell, M.; Odehnal, B.: Convolution surfaces of quadratic triangular Bezier surfaces, *Computer Aided Geometric Design*, 25(2), 2008, 116-129.
- [13] Bastl, B.; Jüttler, B.; Kosinka, J.; Láviccka, M.: Computing exact rational offsets of quadratic triangular Bézier surface patches, *Computer-Aided Design*, 40(2), 2008, 197-209.
- [14] Pottmann, H.: Rational curves and surfaces with rational offsets, *Computer Aided Geometric Design*, 12(2), 1995, 175-192.
- [15] Lü, W.: Offset-rational parametric plane curves, *Computer Aided Geometric Design*, 12(6), 1995, 601-616.
- [16] Farouki, R. T.; Sakkalis, T.: Pythagorean hodographs, *IBM Journal of Research & Development*, 34, 1990, 736-752.
- [17] Farouki, R. T.: *Pythagorean-Hodograph Curves: Algebra and Geometry Inseparable*, Springer, Berlin, 2007.
- [18] Farouki, R. T.; Sederberg, T. W.: Analysis of the offset to a parabola, *Computer Aided Geometric Design*, 12(6), 1995, 639-645.
- [19] Sanchez-Reyes, J.: Offset-rational sinusoidal spirals in Bézier form, *Computer Aided Geometric Design*, 24(3), 2007, 142-150.
- [20] Kim, M.-S.; Park, E.-J.; Lim, S.-B.: Approximation of variable-radius offset curves and its application to Bézier brush-stroke design, *Computer-Aided Design*, 25(11), 1993, 684-698.
- [21] Moon, H. P.: Equivolumetric offsets for 2D machining with constant material removal rate, *Computer Aided Geometric Design*, 25(6), 2008, 397-410.
- [22] Farouki, R. T.; Han, C.Y.; Hass, J.: Boundary evaluation algorithms for Minkowski combinations of complex sets using topological analysis of implicit curves, *Numerical Algorithms*, 40(3), 2005, 251-283.
- [23] Láviccka, M.; Bastl, B.: Rational hypersurfaces with rational convolutions, *Computer Aided Geometric Design*, 24(7), 2007, 410-426.
- [24] Lee, I.-K.; Kim, M.-S.; Elber, G.: Planar curve offset based on circle approximation, *Computer-Aided Design*, 28(8), 1996, 617-630.
- [25] Piegl, L. A.; Tiller, W.: Computing offsets of NURBS curves and surfaces, *Computer-Aided Design*, 31(2), 1999, 147-156.
- [26] Bajaj, C.; Kim, M.-S.: Generation of configuration space obstacles: The case of moving algebraic curves, *Algorithmica*, 4(2), 1989, 157-172.
- [27] Kaul, A.; Farouki, R. T.: Computing Minkowski sums of plane curves, *International Journal of Computational Geometry & Applications*, 5(4), 1995, 413-432.
- [28] Pasko, A.; Okunev, O.; Savchenko, V.: Minkowski sums of point sets defined by inequalities, *Computers & Mathematics with Applications*, 45(10-11), 2003, 1479-1487.
- [29] Rvachev, V. L.: *Methods of Logic Algebra in Mathematical Physics*, (in Russian), Naukova Dumka, Kiev, Ukraine, 1974.
- [30] Shapiro, V.: Real functions for representation of rigid solids, *Computer Aided Geometric Design*, 11(2), 1994, 153-175.
- [31] Mason, J. C. and Handscomb, D.C.: *Chebyshev Polynomials*, Chapman & Hall, Boca Raton, FL, 2003.